Available online at www.sciencedirect.com
ScienceDirect
Lithos 95 (2007) 331–345
LITHOS
www.elsevier.com/locate/lithos

Fluid evolution in the nepheline syenites of the Ditrău Alkaline Massif, Transylvania, Romania

András Fall [a,*], Robert J. Bodnar [a], Csaba Szabó [b], Elemér Pál-Molnár [c]

[a] Fluids Research Laboratory, Department of Geosciences, Virginia Polytechnic Institute and State University, Blacksburg, VA 24061, USA
[b] Lithosphere Fluid Research Laboratory, Department of Petrology and Geochemistry, Eötvös University (ELTE), Pázmány sétány 1/C, H-1117 Budapest, Hungary
[c] Department of Mineralogy, Geochemistry and Petrology, University of Szeged, Egyetem u. 2-6, H-6722 Szeged, Hungary

Received 12 December 2005; accepted 9 August 2006
Available online 9 October 2006

Abstract

The Ditrău Alkaline Massif is an intrusion into the Bucovina nappe system that is part of the Mesozoic crystalline zone located in Transylvania, Romania, in the Eastern Carpathians. Nepheline syenites are the most abundant rocks in the central and eastern part of the Massif, and represent the last major intrusion of the complex. Fluid inclusions in nepheline, aegirine and albite were trapped at magmatic conditions on or below the H_2O-saturated nepheline syenite solidus at about 400–600 °C and 2.5–5 kbars. Early nepheline, and to a lesser extent albite, were altered by highly saline fluids to produce cancrinite, sodalite and analcime, during this process cancrinite also trapped fluid inclusions. The fluids, in most cases, can be modeled by the H_2O–NaCl system with varying salinity; however inclusions with more complex fluid composition (containing K, Ca, CO_3, etc., in addition to NaCl) are common. Raman spectroscopic analyses of daughter minerals confirm the presence of alkali-carbonate fluids in some of the earliest inclusions in nepheline, aegirine and albite.

During crystallization, the melts exsolved a high salinity, carbonate-rich magmatic fluid that evolved to lower salinity as crystallization progressed. Phases that occur early in the paragenesis contain high-salinity inclusions while late phases contain low-salinity inclusions. The salinity trend is consistent with experimental data for the partitioning of chlorine between silicic melt and exsolved aqueous fluid at about 2.0 kbars. The activity of water (a_{H_2O}) in the melt increases during crystallization, resulting in the formation of hydrous phases during late-stage crystallization of the nepheline syenites.
© 2006 Elsevier B.V. All rights reserved.

Keywords: Nepheline syenites; Ditrău Alkaline Massif; Transylvania; Fluid inclusions; Fluid evolution; Raman spectroscopy

1. Introduction

The predominantly nepheline syenitic intrusion of the Ditrău Alkaline Massif (DAM) in Transylvania, Romania, occurs within a rift related continental province. The complex also contains felsic silica-saturated and oversaturated syenites and granites, and ultramafic/mafic rocks. The intrusion has a quasi-circular structure (Fig. 1) and intermediate size (about 800 km^2) with imperfect ring structure and irregular indentations, and is characterized by high alkali and low silica contents, and high volatile and rare earth element contents (Pál-Molnár, 2000). The mineral assemblage is dominated by alkali ferromagnesian silicates, alkali feldspars, nepheline, cancrinite, sodalite

* Corresponding author. Tel.: +1 540 231 9137; fax: +1 540 231 3386.
E-mail address: afall@vt.edu (A. Fall).

0024-4937/$ - see front matter © 2006 Elsevier B.V. All rights reserved.
doi:10.1016/j.lithos.2006.08.005

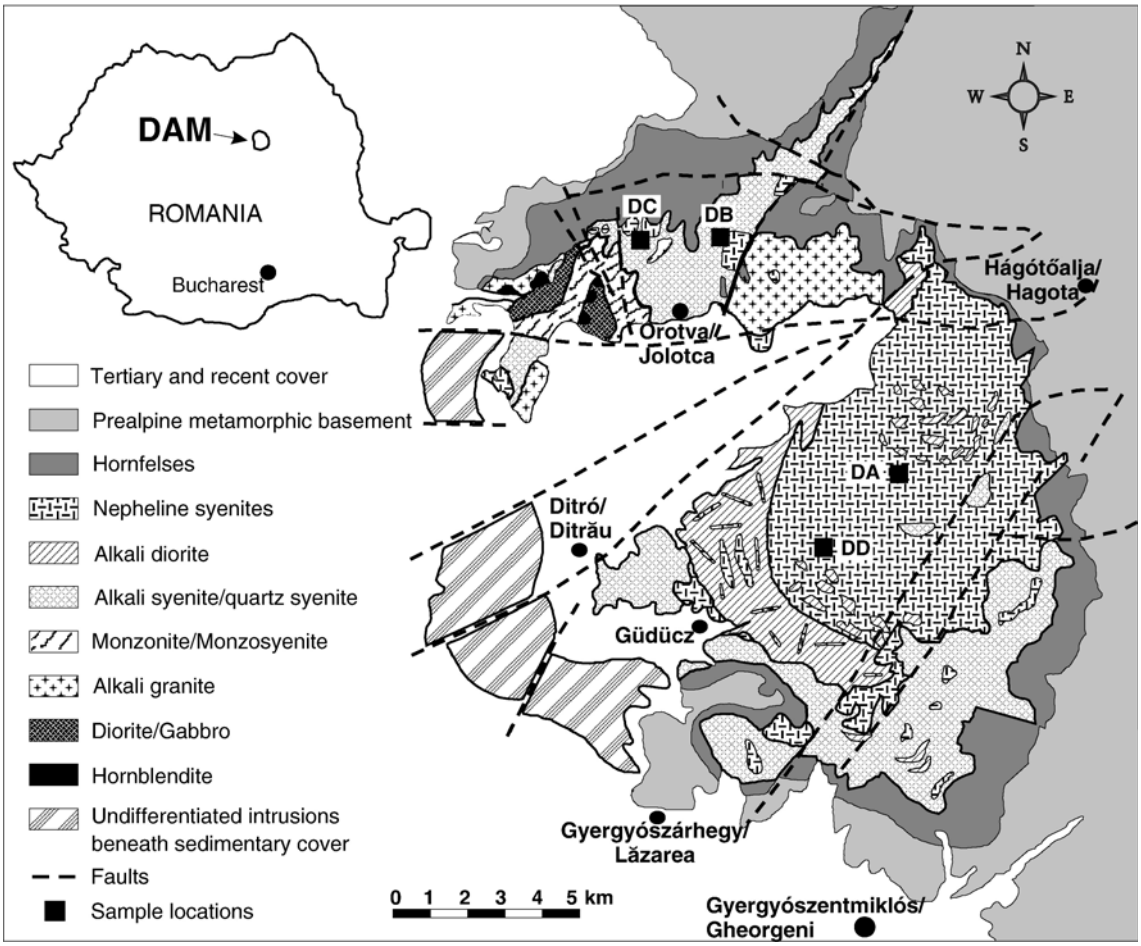


Fig. 1. Location map and geology of the Ditrău Alkaline Massif, with the sample locations: DA — 11 samples; DB — 2 samples; DC — 2 samples, DD — 3 samples. (modified from Kräutner and Bindea, 1998).

and analcime. These features are all characteristics of classic alkaline massifs (Sørensen, 1974).

During crystallization, silicate magmas may become saturated in volatiles and exsolve fluids that include aqueous-carbonic or hydrosaline chloride-rich liquids, among others (Bodnar, 1995; Webster, 2004). The important role that volatiles play during the generation, emplacement and crystallization of alkaline rocks has been emphasized by many authors (Kogarko, 1974; Sobolev et al., 1974; Morogan and Lindblom, 1995; Bühn and Rankin, 1999). The composition and evolution of the volatile phase that exsolves from the melt depends on many factors, including the chemical composition of the silicate melt and the pressure of the system. Fluid inclusions in minerals representing different stages in the paragenesis document the evolving composition of magmatic-hydrothermal fluids in the nepheline syenites of the Ditrău Alkaline Massif.

Pintea (1992) and Pintea and Diamond (1994) described immiscible, hypersaline CO_2–H_2O fluid inclusions in hydrothermal veins associated with REE and MoS_2 mineralization from diorites and hornblendites in the northern part of DAM. The authors also described fluid inclusions containing lower-*T*, high-salinity fluid in nepheline. This latter fluid type is the subject of this study.

2. Geological setting

The DAM in Transylvania, Romania (Fig. 1) is a Mesozoic alkaline igneous complex formed during an extensional phase of the Alpine evolution associated with a rifted continental margin. The massif cuts the Pre-Alpine metamorphic rocks of the Bucovina nappe system near the Neogene-Quaternary volcanic arc of the Calimani–Gurghiu–Harghita Mountain chain (Ianovici,

1938; Kräutner and Bindea, 1998). The nappe system represents the upper unit of the Central Eastern Carpathian nappes, which formed during the Middle Cretaceous (Săndulescu, 1975). The DAM lithology includes a series of ultramafic rocks in the northwest, silica-oversaturated alkaline rock mostly at the northern end, and undersaturated alkaline rocks dominating the central portion and eastern margin of the massif. Numerous dikes, including lamprophyre varieties, tinguaites, microsyenites and nepheline syenite, cut the whole complex.

Starting with the early studies by Herbich (1859) the massif has been the subject of many investigations. However, because of its structural complexity and wide petrographic variability the petrogenesis is still not completely understood, and several petrologic interpretations have been proposed. Streckeisen initially explained the genesis of the massif according to Daly's limestone assimilation theory and later by an origin through magmatic differentiation of alkali syenite parent magma (Streckeisen, 1938, 1960). Anastasiu and Constantinescu (1982) considered a magmatic derivation with two principal rock suites, one generated from a mantle-derived basic magma, and the other from a felsic alkaline magma formed through partial melting of silica-poor crustal rocks. More recently, Kräutner and Bindea (1995, 1998) concluded that the complex formed by three main stages in the Triassic and Jurassic: a) emplacement of a mantle derived gabbro-dioritic magma into the lower crust; b) emplacement of the gabbro-dioritic mass into the crust in a subsolidus stage, magma mixing with a crustal syenitic magma produced a variety of hybrid rocks; c) mantle derived nepheline syenite magma, formed by partial melting, intruded into the Triassic massif, followed by local hydrothermal alteration and mineralization. Pál-Molnár (2000) suggested a two-stage model with the emplacement of ultramafic rocks in the mid-Triassic into the lower crust, with formation of nepheline syenite by fractionation and formation of granites by fractionation and assimilation of silica-rich country rocks. A second stage (middle-Jurassic/lower Cretaceous) involved the emplacement of syenites and diorites. Morogan et al. (2000) suggested a basanitic OIB-like character for the parent magma and that the multistage intrusions were caused by a long-lived mantle plume; they attribute an important role to assimilation and fractionation.

The ultramafic rocks have been dated at about 230 Ma, the gabbros, diorites, monzodiorites, monzonites, syenites and granites are about 215 Ma, and the nepheline syenites have ages of about 165–160 Ma, all determined using K/Ar and $^{40}Ar/^{39}Ar$ chronology (Bagdasarian, 1972; Streckeisen and Hunziker, 1974; Dallmeyer et al., 1997; Kräutner and Bindea, 1998). The final stages of hydrothermal activity and cooling continued until about 115 Ma. Pál-Molnár and Árva-Sós (1995) obtained similar ages for the earlier intrusions, but obtained nepheline ages of about 210–230 Ma and biotite ages of about 180 Ma for the nepheline syenites.

3. Petrography and mineralogy of nepheline syenites

Eighteen samples from four different locations within the massif were collected and examined (Fig. 1). The four samples from the northern part were collected from two nepheline syenite dykes that penetrate the alkali syenites/quartz syenites. The other samples were collected from the nepheline syenite body in the central part of the massif.

The nepheline syenites predominate in the central and eastern part of the massif and are the most abundant rocks of the DAM (Fig. 1). Nepheline syenite containing sodalite, calcite and cancrinite is referred to as "ditroite" in the alkaline rock nomenclature, a term introduced by Zirkel (1866). Recently, Mitchell (1996) proposed the term hypersolvus sodalite nepheline syenite for rocks with the aforementioned mineral composition. On the basis of chemical composition, the nepheline syenites of DAM are characterized as miaskitic because the agpaicity index of the rock (Na+K/Al) varies between 0.8 and 1.0, and Na+K>1/6 Si (Streckeisen and Hunziker, 1974; Sørensen, 1974). The most common variety, the fresh white nepheline syenite, is a coarse- to medium-grained rock that occurs in massive or foliated varieties, and consists of large (5–10 mm) grains of feldspar and nepheline. The mafic components are present in smaller amounts, and include biotite and clinopyroxene, and rarely, amphibole. Other important phases are calcite, cancrinite, sodalite and analcime. Apatite, titanite and zircon are present as accessory phases.

Fig. 2A illustrates the paragenetic relations of major rock forming minerals of the nepheline syenites in the DAM. The mineral paragenesis is very clear, with early magmatic aegirine+albite+nepheline, followed by later magmatic nepheline+perthite+calcite+biotite, and later hydrothermal cancrinite+sodalite+analcime associated with altered nepheline. The feldspars are mostly microcline-perthite and antiperthite (Fig. 3A). Plagioclase with anorthite content of An_4 to An_{28} (Anastasiu and Constantinescu, 1975), corresponding to albite (Fig. 3C), and oligoclase also occur, as prismatic crystals without crystallographic faces, and occasionally as interstitial grains. The clinopyroxene content of the rocks is around 4 vol.% and consists mostly of dark green

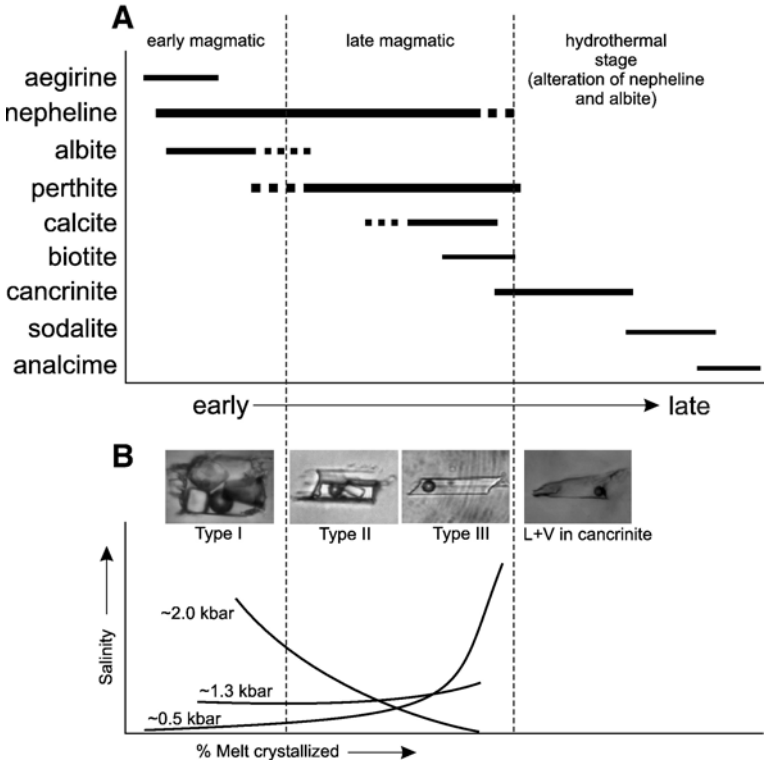


Fig. 2. (A) Paragenesis of major rock forming minerals in nepheline syenites of the Ditrău Alkaline Massif. (B) Salinity of the aqueous fluids exsolved from a crystallizing silicic melt as a function of pressure and crystallization progress. The fluid exsolved at 2.0 kbars has a high initial salinity and decreases as the crystallization progresses (modified from Cline and Bodnar, 1991). The figure also illustrates the relationship between the mineral paragenesis and the salinity evolution of the system, with the various types of fluid inclusions trapped at different stages in the cooling history.

subhedral and anhedral crystals of aegirine (Fig. 3B) and aegirine-augite. The nephelines frequently occur as idiomorphic crystals with hexagonal, short prismatic or square outline, and sometimes as subhedral or anhedral crystals. Textural relations suggest that the euhedral nepheline is early and the anhedral nepheline is a later magmatic phase. The presence of euhedral/subhedral crystals of nepheline (interpreted to be early magmatic phases) as inclusions in perthite (Fig. 3G) demonstrates that nepheline formed earlier than or contemporaneous with perthite. The occurrence of perthite as inclusions in anhedral (late magmatic) nepheline (Fig. 3H) suggests that perthite is a late magmatic phase.

The $(10\bar{1}0)$ cleavage of nepheline crystals is distinct and the hexagonal symmetry is typical of the low temperature (<775 °C) form of nepheline (Hamilton, 1961). The nepheline is often altered to secondary phases including cancrinite, sodalite and analcime (Fig. 3D,E,F). These phases occur as reaction rims, marginal accumulations, crack fillings, or pseudomorphs after nepheline. The presence of cancrinite at the boundary between nepheline and calcite suggests that calcite served as the source of carbonate and calcium needed to produce cancrinite during alteration of nepheline (Fig. 3D). In the northeast of the massif, fresh white nepheline syenites grade into reddish, hydrothermally altered nepheline syenites. The alteration products of nepheline in this area are micaceous aggregates (liebenerite) and smaller amounts of cancrinite (Jakab, 1998).

4. Fluid inclusions

Many studies of fluid and melt inclusions in alkaline massifs have been reported. Most of these are associated with alkaline massifs in the former Soviet Union. A summary of fluid inclusion data (many from nepheline-bearing rocks) was compiled by Sobolev et al. (1974). These workers present fluid inclusion data for nepheline from the Botogol, Nyurgan and Ilmen massifs and Synnyr pluton, as well as for the better known Lovozero and Khibiny classic massifs of the Kola Peninsula, and the Ilímaussaq massif in Greenland, among others. Homogenization temperatures for inclusions considered to be primary in nepheline vary from about 700 to 900 °C; secondary inclusions range from 400 to 600 °C. The salinities range from 20–

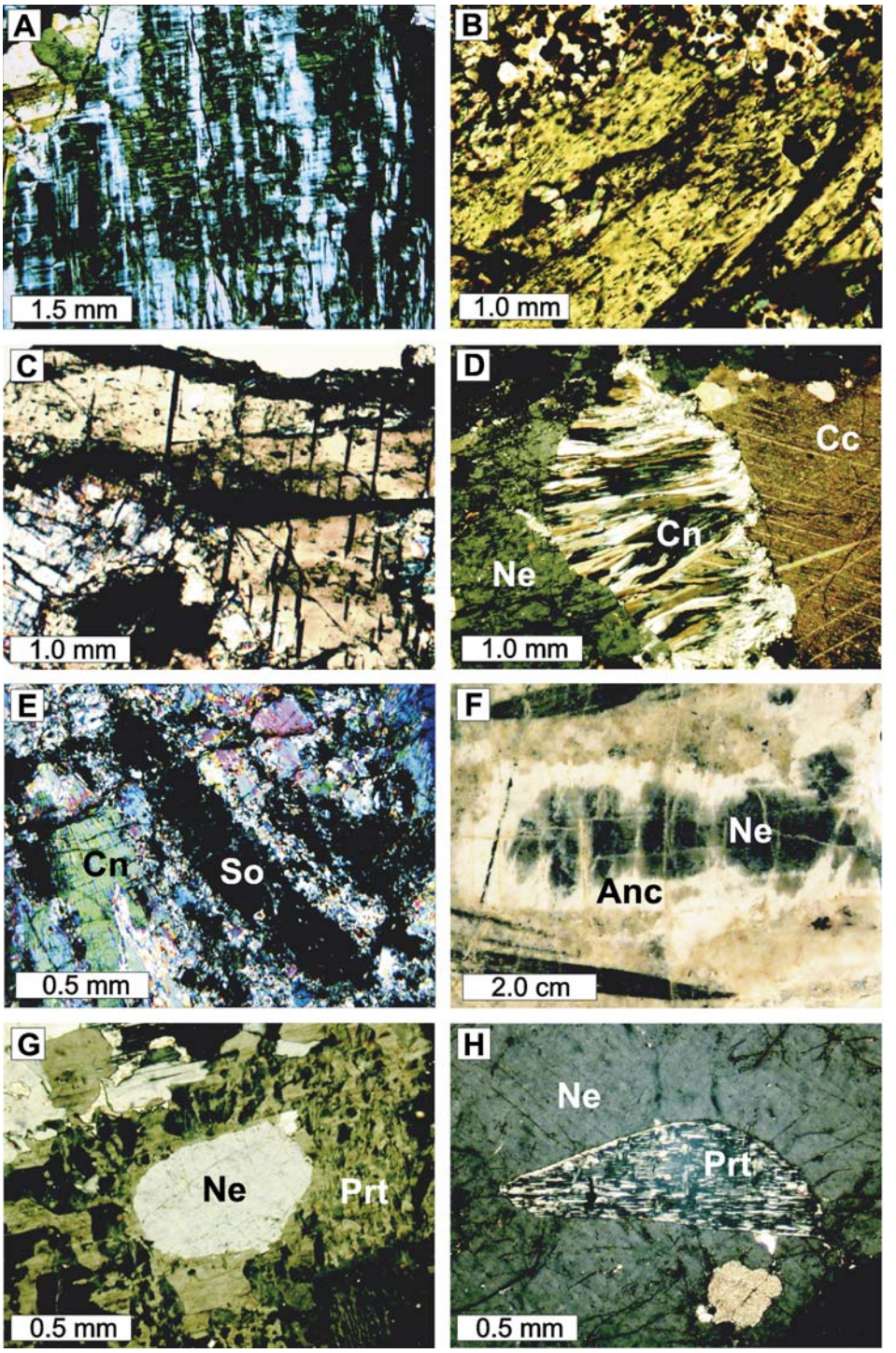


Fig. 3. Mineralogy and textural relations in the nepheline syenites of the Ditrău Alkaline Massif. (A) Microcline-perthite; (B) Aegirine; (C) Albite; (D) Cancrinite (Cn) at the boundary between calcite (Cc) and nepheline (Ne). Calcite serves as the source of carbonate and calcium during alteration of nepheline to produce cancrinite; (E) Cancrinite and interstitial sodalite (So); (F) Analcime (Anc) reaction rim around nepheline. (G) Euhedral/subhedral nepheline inclusion in perthite (Prt). (H) Perthite inclusion in anhedral nepheline. All photos in polarized light.

30 wt.% for the Botogol and Lovozero massifs, and 35–45 wt.% for the Nyurgan and Ilmen massifs. Some of these inclusions contained a number of different alkali-rich daughter minerals and CO_2 was also observed. More recently Potter et al. (2004) and Beeskow et al. (2006) described fluid inclusions in nepheline, eudialyte and sodalite from the nepheline syenites of the Lovozero massif, and from the Khibiny massif, respectively. All of the inclusions were interpreted to be of secondary origin. The inclusions contain a low density CH_4-rich fluid with H_2 and complex hydrocarbons up to C_6H_{12}. In rare occasions these inclusions are associated with aqueous inclusions.

A significant difference between the DAM and the alkaline intrusions described above is that all the above-mentioned massifs formed at a high temperature (600–1000°, or above) and low pressure (1.5–2 kbars), while the DAM formed at lower temperatures (500–700°) and higher pressure (2.5–7 kbars) (Constantinescu and Anastasiu, 1979; Pál-Molnár, 2000).

4.1. Fluid inclusion petrography

Aqueous fluid inclusions interpreted to be primary were observed in nepheline, aegirine, albite and cancrinite in the nepheline syenites of DAM. Definitive evidence for

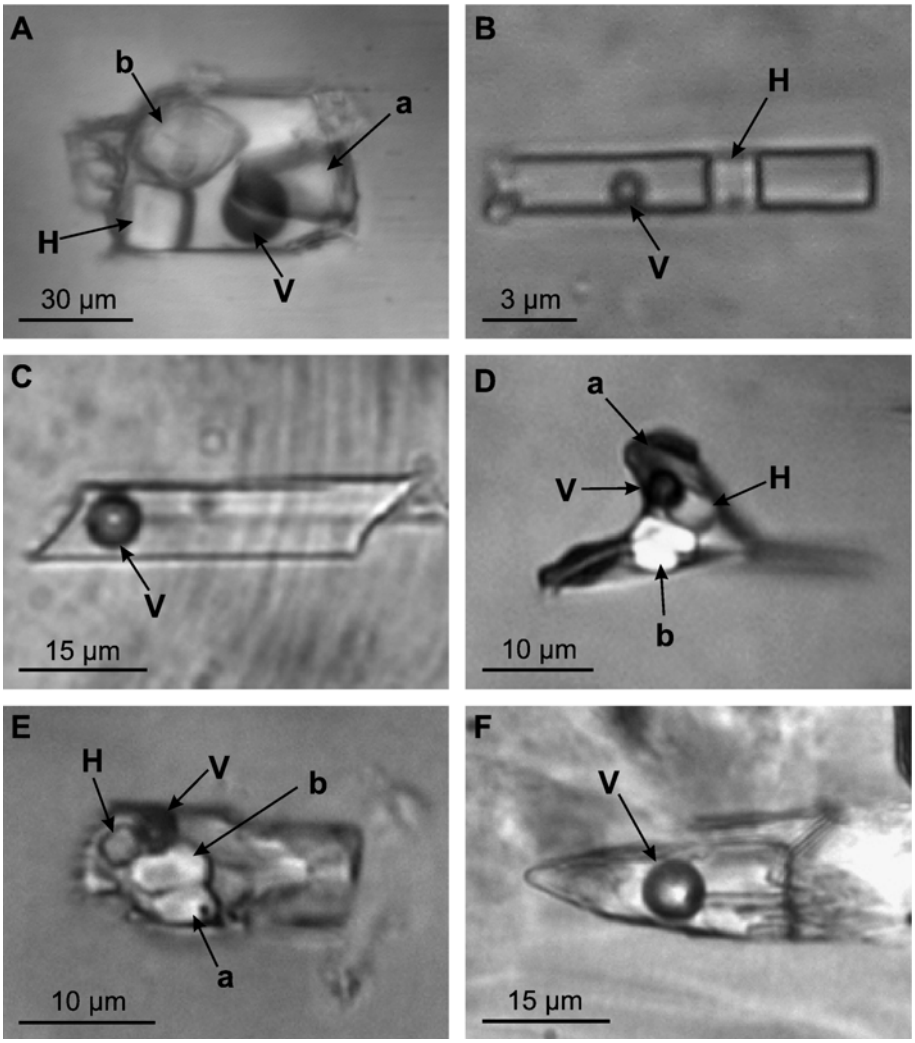


Fig. 4. Photomicrographs of the various fluid inclusion types observed in nepheline syenites of the Ditrău Alkaline Massif. The following symbols apply to all photographs: a — complex hydrated carbonate daughter mineral; b — nahcolite daughter mineral; H — halite; V — vapor. (A) Type I polyphase fluid inclusion (FI) in nepheline. (B) Type II, 3-phase FI in nepheline. (C) Type III, 2-phase FI in nepheline. (D) Polyphase FI in aegirine. (E) Polyphase FI in albite. (F) Type III L–V FI in cancrinite oriented with the "tip" of the inclusion opposite to the crystal growth direction.

primary origin is the occurrence of fluid inclusions along growth zones (Goldstein and Reynolds, 1994; Bodnar, 2003a). Less conclusive is the occurrence of one or a few inclusions in the interiors of minerals, as is the case for most of the inclusions in this study. Even if the inclusions are not primary we can still determine their relative timing in the overall magmatic hydrothermal evolution of the DAM based on mineral paragenesis as described below. Combining information related to timing of mineral or vein formation with types of fluid inclusions contained in minerals from different stages in the paragenesis has been used successfully by other workers to determine fluid evolution (Beane and Titley, 1981; Preece and Beane, 1982; Beane and Bodnar, 1995). Hence, the fluid inclusion paragenesis presented below is based on the mineral paragenetic relationships (Fig. 2A) combined with the types of fluid inclusions observed in minerals from a known position in the paragenesis.

At room temperature the inclusions in nepheline range from polyphase high-salinity inclusions (L+V+solids) to 2-phase low-salinity inclusions (L+V). The large polyphase inclusions (Type I) consist of L+V and 3 or more solid phases (Fig. 4A), and occur randomly, or in small clusters, only in the early stage nepheline. Rarely, intragranular pseudosecondary inclusion trails can be observed. The 3-(Type II) and 2-phase (Type III) inclusions (Fig. 4B,C) occur in clusters, oriented parallel to the cleavage direction (10$\hat{1}$0) of the nepheline. The inclusion size ranges up to 40 μm; in extreme cases the Type I inclusions reach 100 μm. The inclusions typically show negative crystal geometry after the host mineral nepheline or, less frequently, are irregularly shaped.

The Type I polyphase inclusions are considered to be primary based on their distribution within crystals (Bodnar, 2003a). In general, all compositional varieties occur in the early, euhedral nepheline (Fig. 5). However, the late stage (anhedral to subhedral) nepheline contains only Type II or Type III inclusions. The fact that no Type I inclusions are observed in the late-stage nepheline suggests that these fluids were not present during or after formation of the anhedral to subhedral nepheline. As such, when all compositional varieties occur in the same crystal, the Type II and III inclusions are considered younger than Type I inclusions. These crystals are interpreted to have formed early in the paragenesis and fluids representing Type II and III inclusions were trapped later. These later inclusions generally occur along cleavage planes and do not occur along fractures as is more characteristic of secondary inclusions.

Only Type I inclusions (L+V+3 solids) were observed in the aegirine (Fig. 4D) and albite (Fig. 4E). They occur randomly, as individual inclusions, and mostly have irregular shapes. However, some inclusions in albite show negative crystal geometry after the host mineral. The inclusions are less abundant and smaller than in nepheline, ranging up to 20 μm.

The cancrinite contains Type III 2-phase (L+V) inclusions (Fig. 4F) and most of the inclusions have a

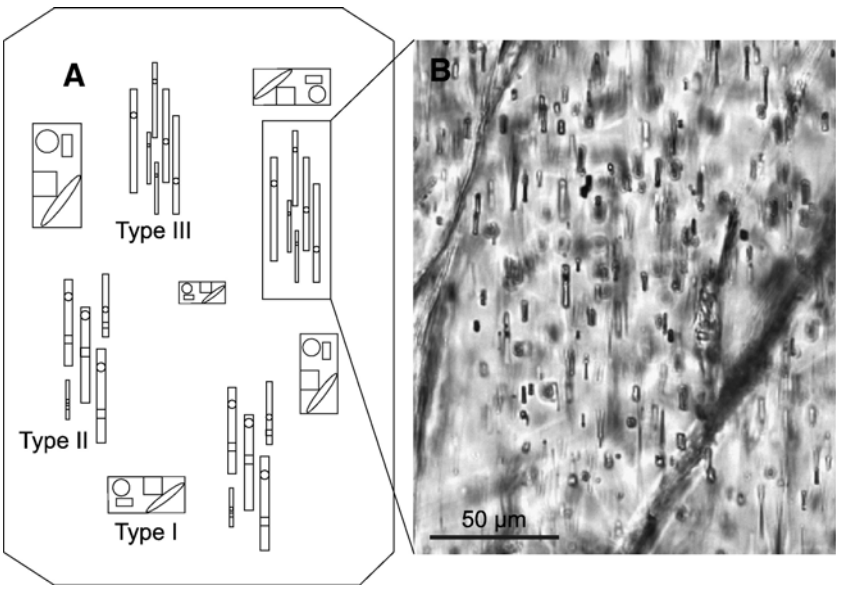


Fig. 5. (A) Sketch showing the different compositional varieties of fluid inclusions that occur in nepheline and their general distribution. (B) Photomicrograph of a three-dimensional Type III fluid inclusion assemblage, with inclusions oriented along the (10$\bar{1}$0) cleavage direction of nepheline.

Table 1
Summary of microthermometric data from fluid inclusions from nepheline syenites of the Ditrău Alkaline Massif

FI type	Aegirine	Albite	Nepheline			Cancrinite
	Type I (n=21)	Type I (n=28)	Type I (n=54)	Type II (n=118)	Type III (n=135)	Type III (n=42)
T_h	151–160	148–164	148–161	250–315	243–305	180 to 230
T_{ms1}	139–147	139–148	138–148			
T_{ms2}	1790–186	174–186	173–187			
T_{mH}	280–320	272–324	277–325	264–325		
T_{mi}					−17.3 to −20.7	−3.7 to −6.3
S				35.5 to 39.8	20.5 to 22.9	6.0 to 9.6

Abbreviations: T_h — homogenization temperature (°C); T_m — melting temperature (°C); i — ice; s_1 — daughter mineral 1 (complex hydrated carbonate); s_2 — daughter mineral 2 (nahcolite); H — halite; S — salinity (wt.% NaCl eqv.); FI — fluid inclusion; n — number of fluid inclusions.

specific elongated triangular shape. The "tip" of the inclusions faces opposite to the growth direction of the host mineral. The sizes of the inclusions range up to 25 μm.

4.2. Microthermometry

Fluid inclusion petrography and microthermometry were conducted using doubly polished thin sections (80–120 μm thick) of nepheline syenite. The microthermometric analyses were conducted on a Linkam THMSG 600 heating-freezing stage and a Fluid Inc. USGS type gas-flow stage, both calibrated using synthetic fluid inclusion standards (Sterner and Bodnar, 1984). The inclusions were chosen to be representative of fluid inclusions assemblages (FIA) within the host mineral (Goldstein and Reynolds, 1994). Because the host minerals have well-developed cleavage that could lead to leakage (Bodnar, 2003c) the inclusions first were cooled and then heated to homogenization. Type I inclusions were only heated because of their complex nature which precluded interpretation of low temperature behavior. However, heating of these inclusions provided information on the dissolution properties of the different solid phases. This information was useful in the identification of phases during Raman spectroscopic analysis, as described below.

The composition and salinity of Types II and III (including low-salinity cancrinite-hosted) fluid inclusions were determined from halite dissolution and ice-melting temperatures, respectively, using the equations of Bodnar (1993, 2003b) and Sterner et al. (1988). Initial ice-melting of Type III inclusions was between −23 and −21 °C, therefore these inclusions were interpreted using the H_2O–NaCl system because this temperature is near the eutectic temperature for the system H_2O–NaCl (Bodnar, 1993). Ice-melting temperatures of Type III inclusions in nepheline ranged from −17.3 to −20.7 °C, corresponding to salinities between 20.5 and 22.9 wt.% NaCl equivalent. Homogenization temperatures ranged from 243 to 305 °C. Ice-melting temperatures of inclusions in cancrinite ranged from −3.7 to −6.3 °C, corresponding to salinity of 6.0 to 9.6 wt.% NaCl equivalent, and the inclusions homogenize between 180 and 230 °C. Halite dissolution temperatures of Type II inclusions ranged from 264 to 325 °C, corresponding to salinities from 35.5 to 39.8 wt.% NaCl equivalent, based on the equations of Sterner et al. (1988). The vapor bubbles in Type II inclusions disappeared (250–315 °C) before the halite, and the inclusions often decrepitated before the halite dissolved as a result of the high pressures generated in the inclusions during heating (Bodnar, 1994). The microthermometric results are summarized in Table 1 and the relationship between salinity and homogenization temperature for the different inclusion types is shown on Fig. 6.

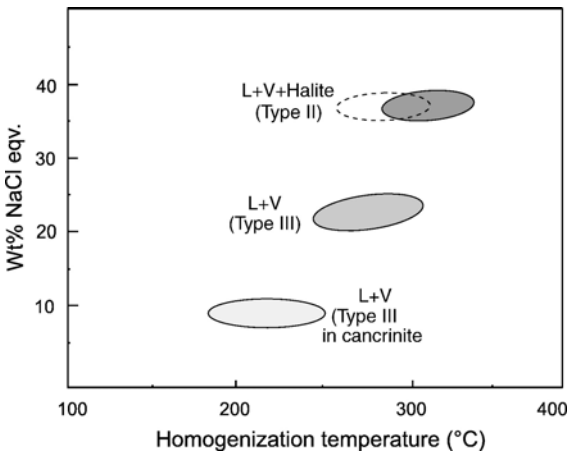


Fig. 6. Relationship between salinity and homogenization temperature for the various H_2O–NaCl fluid inclusion types studied. Type II inclusions homogenize by halite dissolution after the bubble disappearance. Bubble disappearance temperatures for Type II inclusions are shown by the dashed-line field.

4.3. Raman spectroscopy

Daughter minerals in the Type I inclusions were identified by Raman spectroscopic analyses. Analyses were conducted using a JY Horiba HR800 LabRAM Raman microprobe equipped with an electronically cooled charge-coupled device (CCD) detector, using 514.57 nm (green) Ar-ion laser excitation, operated in confocal mode with the aperture set to 150 μm. The laser was focused through an Olympus UPLAPO 60× objective (NA = 0.9, working distance = 0.2 mm above cover glass; Adar et al., 2004). The acquisition time varied from 30 to 60 s, but was increased to 10 min for some weaker signals. The samples were orientated to provide the maximum intensity for the peaks of interest, owing to the polarized nature of the laser which causes significant differences in the spectra as a function of crystal orientation (Burke, 2001).

The Type I inclusions contain 3 or more solid phases, and are described here in the order in which they dissolve during heating. The first solid is a tabular, elongated, anisotropic phase that dissolved at about 138–148 °C. Raman spectra display two fundamental vibrations at 152 and 1063 cm^{-1} (Fig. 7A) that correlate most closely with thermonatrite (156 and 1062 cm^{-1}, $Na_2CO_3 \cdot H_2O$), trona (164 and 1060 cm^{-1}, $Na_3(CO_3)(SO_4)_2$) or gaylussite (164 and 1071 cm^{-1}, $Na_2Ca(CO_3)_2 \cdot 5H_2O$). Based on its dissolution properties (Lipin, 2001), this phase is probably thermonatrite mixed with the other above mentioned phases, and can be considered to be a complex hydrated carbonate. The second solid is a tabular, anisotropic phase that dissolved around 173–187 °C. The Raman spectrum displays fundamental vibrations at 145, 685, 1045, 1266 and 1434 cm^{-1} (Fig. 7B). This phase was identified as the sodium bicarbonate nahcolite ($NaHCO_3$). All Type I inclusions contained a cubic, isotropic phase that showed a very weak Raman signal or no signal at all, and was identified as halite after the optical and dissolution properties (dissolved around 272–325 °C).

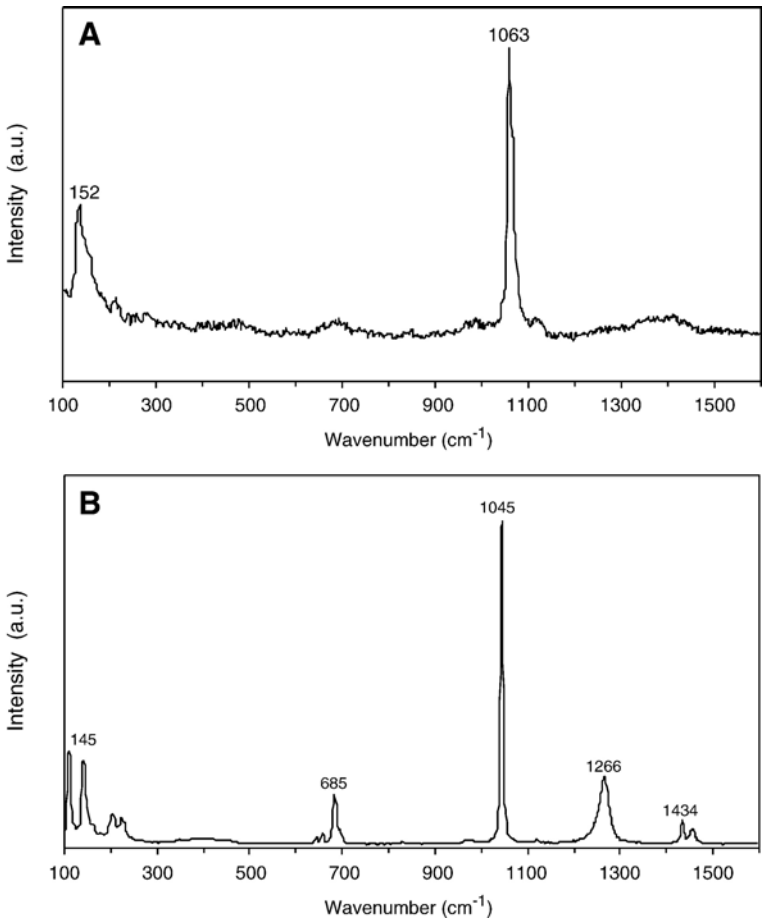


Fig. 7. Raman spectra of (A) a complex hydrated carbonate daughter mineral and (B) a nahcolite daughter mineral observed in Type I fluid inclusions.

A few inclusions contained phases that showed Raman peaks at 157, 286, 715 and a very strong peak at 1089 cm^{-1}. This phase was identified as a complex anhydrous carbonate that dissolved around 175–180 °C. Muscovite was also identified during Raman analyses. This phase is probably a trapped solid, as evidenced by its random occurrence and by the fact that it did not dissolve during heating.

5. Discussion

The occurrence of primary fluid inclusions in magmatic phenocrysts and alteration phases in the nepheline syenites of the DAM is direct evidence that a fluid was present during the formation of the rock. The minerals trapped diverse fluid inclusion populations with varied compositions and salinities, documenting a decrease in salinity during crystallization. It should be noted, however, that coexisting melt and aqueous inclusions that are commonly observed in systems involving aqueous fluid-melt immiscibility (Student and Bodnar, 1999, 2004; Bodnar and Student, 2006) have not been observed in the Ditrău Massif.

Aegirine, nepheline and albite occur as early phases, followed by microcline-perthites, biotite and amphibole, followed by calcite and finally the secondary phases cancrinite, sodalite, and analcime. The early phases trapped high-salinity fluids and the late phases (late stage nepheline and cancrinite) trapped lower salinity fluids. The fact that the early mineral phases contain primary fluid inclusions suggests that the nepheline syenitic melt was saturated in water relatively early in the crystallization history.

The nepheline–kalsilite–silica (Ne–Ks–Qz) diagram is a commonly used geothermometer (Hamilton and MacKenzie, 1960; Hamilton, 1961; Platt, 1996), because the amounts of kalsilite and silica that can be incorporated into nepheline vary with temperature (Fig. 8). Nepheline compositions of the DAM (Constantinescu and Anastasiu, 1979; Morogan et al., 2000) plotted on the Ne–Ks–Qz diagram indicate crystallization temperatures in the range 500–700 °C and fall close to the low-temperature Morozewicz–Buerger convergence field (Tilley, 1954; Platt, 1996) that represents slowly cooled plutonic nepheline syenites.

Isochores representing the minimum and maximum homogenization temperatures of the Type III inclusions (21 wt.% NaCl eqv., 245–305 °C isochores) and inclusions in cancrinite (7 wt.% NaCl eqv., 180–230 °C isochores) are plotted on Fig. 9 along with the calculated temperature of crystallization of nepheline, and the H_2O-saturated and H_2O+CO_2-saturated nepheline syenite solidi (Millhollen, 1971). The intersection of the isochore field for Type III inclusions with the formation temperature range of nepheline from Fig. 8 constrains the trapping conditions of inclusions in nepheline (Roedder and Bodnar, 1980). This intersection defines a lower pressure of about 2.5 kbars, close to the value (2.0 kbars) used by Hamilton (1961) for his experiments on nepheline solid solutions. The upper pressure limit of 5.0 kbars is estimated from the position of DAM relative to the units of the Bucovina nappe system penetrated by the massif, which suggest that the melt crystallized not deeper than about 15 km. The deep crustal level is supported by the long isobaric cooling history, which lasted about 20–25 Ma (Kräutner and Bindea, 1998). According to this, crystallization of secondary phases occurred approximately in the same pressure range as the nepheline, only at lower temperatures. Hence, the P–T trapping conditions of inclusions in cancrinite can be estimated from the intersection of the isochore field with the pressure range up to 5.0 kbars (Fig. 9). The H_2O-saturated nepheline syenite solidus is most applicable to the present system. Although carbonates are common in the fluid inclusions in the nepheline syenites, CO_2-bearing inclusions are found in the diorites and hornblendites (Pintea, 1992; Pintea and Diamond, 1994), and the presence of molecular CO_2 in the cancrinite-sodalite mineral group was confirmed (Della Ventura et al., 2005), no CO_2 was observed in fluid inclusions from the nephelines syenites.

The results shown on Fig. 9 suggest that cancrinite was formed in the subsolidus region during alteration of nepheline associated with post-magmatic hydrothermal activity. It is well known from studies of porphyry copper deposits that mixing of magmatic and meteoric water plays an important role in the alteration process during the hydrothermal stage (Beane and Titley, 1981; Beane and Bodnar, 1995). Mixing of magmatic and meteoric water decreases the salinity of hydrothermal fluids. Paragenetic information suggests that cancrinite was formed late and in the subsolidus region (Fig. 9) by alteration of nepheline and fluid inclusions in cancrinite show lower salinity compared to those in nepheline. We interpret the lower salinity fluids associated with cancrinite formation to be the result of mixing of late magmatic fluids with meteoric water.

The partitioning of chlorine between the silicic melt and the exsolving aqueous fluid is pressure dependent (Fig. 2B, Cline and Bodnar, 1991). At pressures below about 1.3 kbars, the salinity of the earliest magmatic fluid is low and the salinity of the exsolving fluid increases during crystallization. In deeper (higher pressure) systems the first fluid exsolved from the melt has high salinity and salinity decreases as

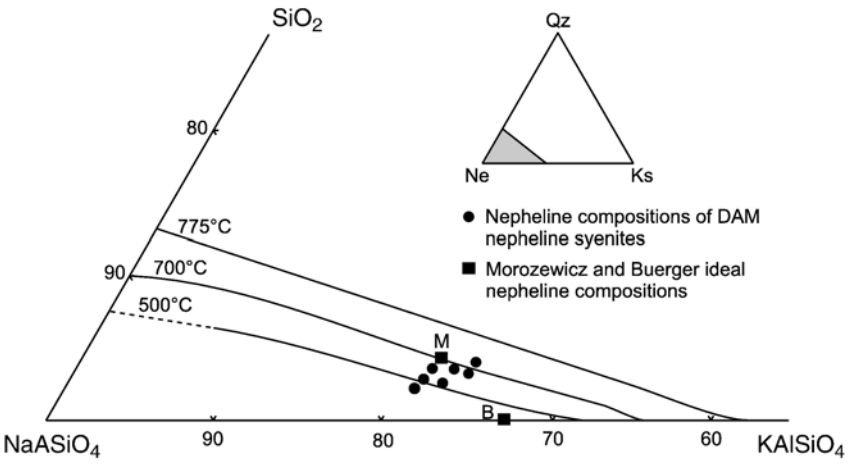


Fig. 8. Compositions of nepheline from the DAM nepheline syenites (data of Constantinescu and Anastasiu, 1979; Morogan et al., 2000) plotted on the nepheline–kalsilite–silica diagram. Isotherms show the limits of nepheline solid solution at various temperatures (modified from Hamilton, 1961). Nephelines from the DAM fall mostly between the 500 and 700 °C isotherms. Ideal nepheline compositions from Morozewicz (M) and Buerger (B) are also shown (Tilley, 1954; Platt, 1996).

crystallization proceeds. Phase equilibria confirm a minimum pressure of formation for the DAM nepheline syenites of about 2.5 kbars. As a result the first exsolved fluids at higher pressures (~ 2 kbars, Fig. 2B) would have the highest salinity, and fluid salinity would decrease as crystallization progressed. The salinity of magmatic fluid predicted from theoretical and experimental studies described above is consistent with the observed temporal variation in fluid inclusion salinity in the DAM.

The decreasing salinity observed in the DAM is consistent with formation of late primary and secondary phases mostly by alteration of nepheline (and albite). The observed alteration of nepheline by low-temperature hydrothermal fluids in the temperature range 400–500 °C is consistent with experimental results of Boettcher and Wyllie (1969). Calcite crystallizes as a late primary (magmatic) phase, removing most of the carbonate from the fluid. In the subsolidus region, nepheline is altered to cancrinite, removing additional carbonate and chlorine and sulfate from the fluid. In situations where cancrinite is formed at the grain boundary between nepheline and calcite, calcite serves as the source of carbonate and calcium to form cancrinite (Fig. 3D). Nepheline and, to a lesser extent, albite are altered to sodalite, removing NaCl from the fluid in the process. Albite alteration generates silica that reacts with nepheline to form analcime. The reactions describing the alteration processes are summarized in Table 2.

As mentioned above, in order to trap primary aqueous fluid inclusions in early crystallizing phases the melt must be saturated in water early in the crystallization history. The solubility of water in the melt depends mostly on the melt composition (i.e., silica content, alkali/aluminum ratio of the melt) and the pressure of the system (Dingwell et al., 1984). Dingwell et al. (1984) note that phonolitic melts (with compositions similar to the nepheline syenites of the DAM)

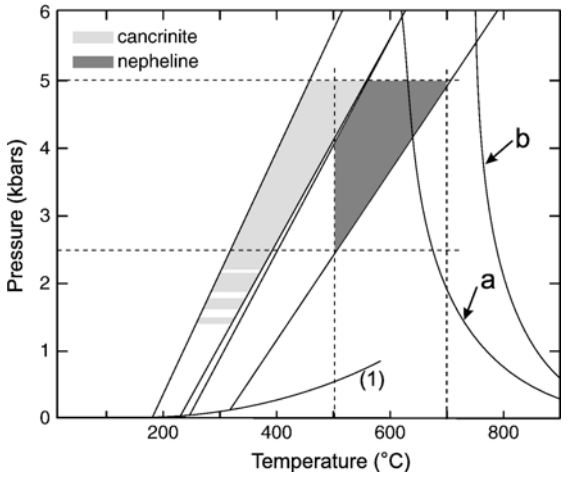


Fig. 9. *P–T* diagram showing the isochores for the Type III fluid inclusions in nepheline with an average salinity of 21 wt.% NaCl eqv., and for inclusions in cancrinite with an average salinity of 7 wt.% NaCl eqv. Curve (1) is the liquid-vapor phase boundary for the described compositions. The dashed lines show the estimated *P–T* conditions of crystallization of nepheline in the DAM. The estimated trapping conditions of inclusions in cancrinite are also shown in the shaded regions. The H_2O-saturated (a) and H_2O+CO_2-saturated (b) nepheline syenite solidi are from Millhollen (1971).

Table 2
Reactions describing alteration of nepheline and albite to cancrinite, sodalite, and analcime

$$6\ \underset{\text{nepheline}}{NaAlSiO_4} + 2\ \underset{\text{complex carbonate}}{Ca(Cl_2, CO_3, SO_4)} + \underset{\text{fluid}}{H_2O} = \underset{\text{cancrinite}}{Na_6Ca_2(AlSiO_4)_6(Cl_2, CO_3, SO_4)_2 \cdot H_2O}$$

$$6\ \underset{\text{nepheline}}{NaAlSiO_4} + 1.5\ \underset{\text{calcite}}{CaCO_3} + 1.1\underset{\text{fluid}}{H_2O} = \underset{\text{cancrinite}}{Na_6Ca_{1.5}(AlSiO_4)_6(CO_3)_{1.5} \cdot 1.1\ H_2O}\ ^{a}$$

$$6\ \underset{\text{nepheline}}{NaAlSiO_4} + 2\ \underset{\text{from fluid}}{NaCl} = \underset{\text{sodalite}}{Na_8(AlSiO_4)_6Cl_2}$$

$$6\ \underset{\text{albite}}{NaAlSi_3O_8} + 2\ \underset{\text{from fluid}}{NaCl} = \underset{\text{sodalite}}{Na_8(AlSiO_4)_6Cl_2} + 12\ \underset{\text{silica in fluid}}{SiO_2}$$

$$\underset{\text{nepheline}}{NaAlSiO_4} + \underset{\text{from fluid}}{H_4SiO_4} = \underset{\text{analcime}}{NaAlSi_2O_6 \cdot H_2O} + H_2O$$

[a] For the pure carbonate end-member of cancrinite, as suggested by experimental studies of the breakdown of cancrinite by Sîrbescu and Jenkins (1999).

show enhanced water solubility compared to silica-saturated melts. According to their data, the solubility of water in granites at 660–810 °C and 1 kbar is about 3.0–3.2 wt.% H_2O, and the solubility increases with increasing pressure to about 8.0 wt.% H_2O at 5 kbars. At 1 kbar and this same temperature range the solubility of water in phonolitic melt is about 5.0 wt.%, and extrapolating to 3.5 kbars indicates approximately 7 wt.% H_2O. Similarly, Carroll and Blank (1997) demonstrated that phonolitic melts are capable of incorporating significantly more dissolved H_2O at a given pressure than basaltic or rhyolitic melts. According to their results, phonolitic melts contain about 4.5–4.8 wt.% H_2O at 1 kbar and 850 °C. Extrapolating to higher pressures, H_2O solubility in the melt at about 5 kbars can reach approximately 10.0 to 12.0 wt.%. Considering these data, if the nepheline syenite of the Ditrău Massif crystallized at 5 kbars and 700 °C, the melt could have contained up to about 10.0 wt.% H_2O. As the melt crystallized a highly saline fluid phase exsolved and is preserved as fluid inclusions in the early nepheline, albite and aegirine.

Biotite and amphibole occur as late phases in the nepheline syenites, and the formation of these hydrous silicates can be related to the activity of water (a_{H_2O}) in the system. The a_{H_2O} in the aqueous phase can be calculated from the fluid salinity. If we assume ideal behavior, the a_{H_2O} is equal to the mole fraction of water (X_{H_2O}). The mole fraction of H_2O in an H_2O–NaCl solution can be calculated according to Eq. (1):

$$X_{H_2O} = \frac{\frac{m_{H_2O}}{MW_{H_2O}}}{\frac{m_{H_2O}}{MW_{H_2O}} + \frac{m_{NaCl}}{MW_{NaCl}}} \quad (1)$$

where m_{H_2O} and m_{NaCl} are the masses of H_2O and NaCl in the solution, respectively, and MW_{H2O} and MW_{NaCl} are the molecular weights of H_2O and NaCl, respectively. According to Eq. (1), the a_{H_2O} in a 39.8 wt.% NaCl solution (the highest salinity recorded by Type II inclusions) is 0.83, and the activity of water increases with decreasing salinity. For a salinity of 6.0 wt.% NaCl (the lowest salinity recorded by inclusions in cancrinite) the a_{H_2O} is 0.98. The water activity increase reflects the combined effects of decreasing salinity of the exsolved magmatic fluid with time as well as mixing of high salinity magmatic fluids with lower salinity meteoric waters.

Experimental data of Aranovich and Newton (1996) show that the activity of H_2O at 640 °C and 2 kbars in a concentrated NaCl solution is close to that of an ideal solution. At these conditions, $a_{H_2O} = X_{H_2O} - 0.008$. At higher pressures the difference between the activity and mole fraction increases, reaching about 0.19 units at 10 kbars and same temperature. Using these values and assuming a linear relationship between activity and mole fraction between 2 and 10 kbars, we estimate that the activity of water in the magmatic fluid at 3.5 kbars is: $a_{H_2O} = X_{H_2O} - 0.042$.

The partitioning of chlorine between granitic melt and coexisting aqueous phase is pressure dependent (Kilinc and Burnham, 1972). This trend also applies to phonolitic melts (Signorelli and Carroll, 2000). We have assumed a partition coefficient of 0.01, which corresponds to a pressure of about 3.5 kbars (Shinohara et al., 1989). Because we know the concentration of Cl in the aqueous phase and the partition coefficient, we can estimate the concentration of Cl in the melt. As noted previously, the solubility of water in a nepheline syenite melt at 3.5 kbars is approximately 7 wt.%, and the fluid inclusion evidence suggests that the melt was saturated in H_2O during much of its crystallization history. Burnham and Davis (1971, 1974) showed experimentally that in the pure albite–H_2O system the activity of water in the silicate melt is equal to the activity of water in the coexisting aqueous phase. Using the chlorine concentration in the melt and the solubility of H_2O in the nepheline syenite melt, the mole fractions of (Na)Cl and H_2O in the melt and fluid were estimated, and the activity of H_2O in both phases was calculated as described above, using the relationship between mole fraction and activity reported by Aranovich and Newton

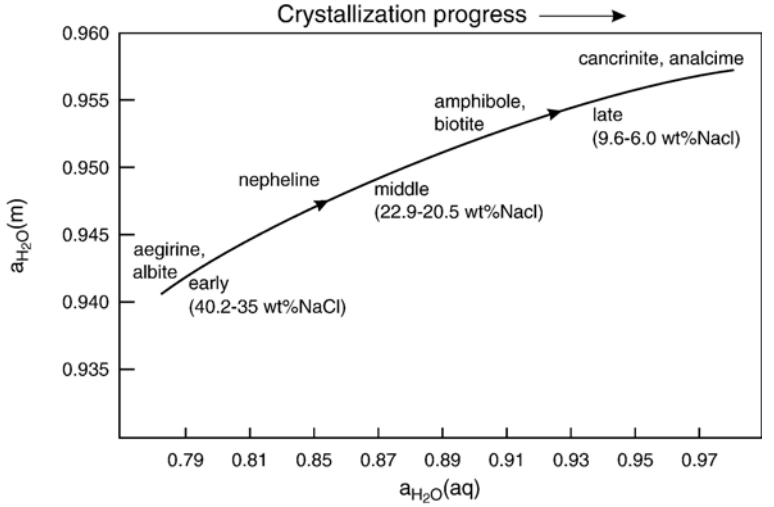


Fig. 10. Relationship between the activity of H_2O in the melt (a_{H_2O}(m)) and the activity of H_2O in the coexisting aqueous solution (a_{H_2O}(aq)). Also shown is the mineral and fluid paragenesis during crystallization of the nepheline syenites of DAM.

(1996). The variation in the activity of H_2O in the aqueous and melt phases, along with the mineral paragenesis and evolution in fluid salinity during crystallization, are shown in Fig. 10. Note that the activity of water in the melt and aqueous phases both increase during crystallization, consistent with the appearance of the hydrous phases biotite and amphibole late in the paragenesis.

6. Conclusions

The parent melt of the nepheline syenites of the Ditrău Alkaline Massif became saturated in an alkali–carbonate-rich aqueous fluid early in the crystallization history. This interpretation is consistent with the fractionation residua origin for the nepheline syenite melt (Pál-Molnár, 2000; Morogan et al., 2000). Primary fluid inclusions from different stages in the paragenesis provide direct evidence for the presence of aqueous solutions. The fluid inclusion compositions range from a highly saline, carbonate-rich end member, producing a varied assemblage of daughter minerals, to a low-salinity, NaCl-rich end member. The diverse fluid inclusion populations document a decrease in the salinity of the magmatic-hydrothermal fluid during crystallization. The decrease in salinity is consistent with formation of primary mineral phases that remove Cl, CO_3 and SO_4 from the aqueous solution, or secondary phases formed by alteration of either nepheline or albite, or both, according to the following model. Crystallization of calcite as a late primary phase removes carbonate from the solution. Alteration of nepheline to cancrinite removes additional carbonate, as well as Cl and SO_4. The formation of sodalite by alteration of nepheline (or albite) removes NaCl from the aqueous solution. The alteration of albite to produce sodalite also releases silica to the solution, which is used in the alteration of nepheline to produce analcime. Late crystallization of the hydrous minerals biotite and amphibole is related to increasing activity of water in the melt and in the coexisting aqueous phase. This interpretation suggests that the nepheline syenite melt achieved volatile saturation soon after crystallization began, and that an active magmatic hydrothermal system existed during much of the crystallization history of the nepheline syenites of the Ditrău Alkaline Massif.

Acknowledgements

The authors thank István Márton, Judit Gál, Éva Benő, Kálmán Török and Péter Luffi for their assistance during this study. Mr. Charles Farley assisted with Raman analysis in the Fluids Research Laboratory at Virginia Tech. The suggestions and comments of Michael Marks (Tübingen) and an anonymous reviewer are highly appreciated and contributed significantly to the improvement of the paper. Partial funding for this research was provided by Lithosphere Fluid Research Laboratory (Budapest, HU), grants from the U.S. National Science Foundation to R.J. Bodnar (Grant EAR-0125918) and from the Hungarian National Science Foundation to E. Pál-Molnár (Grant No. T046736).

This is the No. 34 publication of the Lithosphere Fluid Research Laboratory (LRG) at Eötvös University in collaboration with the Fluids Research Lab at Virginia Tech.

References

Adar, F., Naudin, C., Whitley, A., Bodnar, R.J., 2004. Use of a microscope objective corrected for a cover glass to improve confocal spatial resolution inside a sample with a finite index of refraction. Appl. Spectrosc. 58, 1136–1137.

Anastasiu, N., Constantinescu, E., 1975. On the mineralogy of syenites from the alkaline massif of Ditrău. Com. Geol., Buc. 77–85.

Anastasiu, N., Constantinescu, E., 1982. Tectonostructural position of the foidic rocks in the Romanian Carpathians. Rev. Roum. Geol. 26, 33–45.

Aranovich, L.Ya., Newton, R.C., 1996. H_2O activity in concentrated NaCl solutions at high pressures and temperatures measured by the brucite-periclase equilibrium. Contrib. Mineral. Petrol. 125, 200–212.

Bagdasarian, G.P., 1972. Despre vârsta absolută a unor roci eruptive şi metamorfice din masivul Ditrău şi Munţii Banatului din România. Stud. Cercet. Geol. Geofiz. Geogr., Ser. Geol. XVII/1, 13–21.

Beane, R.E., Titley, S.R., 1981. Porphyry copper deposits. Part II. Hydrothermal alteration and mineralization. Econ. Geol. 75th Anniversary volume, 235–269.

Beane, R.E., Bodnar, R.J., 1995. Hydrothermal fluids and hydrothermal alteration in porphyry copper deposits. In: Pierce, F.W., Bohm, J.G. (Eds.), Porphyry Copper Deposits of the American Cordillera. Arizona Geological Society Digest, vol. 20, pp. 83–93. Tucson, AZ.

Beeskow, B., Treloar, P.J., Rankin, A.H., Vennemann, T.W., Spangenberg, J., 2006. A reassesment of models for hydrocarbon generation in the Khibiny nepheline syenite complex, Kola Peninsula, Russia. Lithos 91, 1–18.

Bodnar, R.J., 1993. Revised equation and table for determining the freezing point depression of H_2O–NaCl solutions. Geochim. Cosmochim. Acta 57, 683–684.

Bodnar, R.J., 1994. Synthetic fluid inclusions: XII. The system H_2O–NaCl. Experimental determination of halite liquidus and isochores for a 40 wt.% NaCl solution. Geochim. Cosmochim. Acta 58, 1053–1063.

Bodnar, R.J., 1995. Fluid inclusion evidence for a magmatic source for metals in porphyry copper deposits. In: Thompson, J.F.H. (Ed.), Magmas, Fluids and Ore Deposits. Mineral. Assoc. of Can. Short Course, vol. 23, pp. 139–152.

Bodnar, R.J., 2003a. Introduction to fluid inclusions. In: Samson, I., Anderson, A., Marshall, D. (Eds.), Fluid Inclusions: Analysis and Interpretation. Mineral. Assoc. Can. Short Course, vol. 32, pp. 1–8.

Bodnar, R.J., 2003b. Interpretation of data from aqueous-electrolyte fluid inclusions. In: Samson, I., Anderson, A., Marshall, D. (Eds.), Fluid Inclusions: Analysis and Interpretation. Mineral. Assoc. Can., Short Course, vol. 32, pp. 81–99.

Bodnar, R.J., 2003c. Reequilibration of fluid inclusions. In: Samson, I., Anderson, A., Marshall, D. (Eds.), Fluid Inclusions: Analysis and Interpretation. Mineral. Assoc. Canada, Short Course, vol. 32, pp. 213–230.

Bodnar, R.J., Student, J.J., 2006. Melt inclusions in plutonic rocks: petrography and microthermometry. In: Webster, J.D. (Ed.), Melt Inclusions in Plutonic Rocks. Mineral Assoc. Canada, Short Course, vol. 36, pp. 1–26.

Boettcher, A.L., Wyllie, P.J., 1969. Phase relationships in the system $NaAlSiO_4$–SiO_2–H_2O to 35 kilobar pressure. Am. J. Sci. 267, 875–909.

Burke, E.A.J., 2001. Raman microspectroscopy of fluid inclusions. Lithos 55, 139–158.

Burnham, C.W., Davis, N.F., 1971. The role of water in silicate melts. I. *P–V–T* relations in the system $NaAlSi_3O_8$–H_2O to 10 kilobars and 1000 °C. Am. J. Sci. 270, 54–79.

Burnham, C.W., Davis, N.F., 1974. The role of water in silicate melts. II. Thermodynamic and phase relations in the system $NaAlSi_3O_8$–H_2O to 10 kilobars, 700° to 1100 °C. Am. J. Sci. 274, 902–940.

Bühn, B., Rankin, A.H., 1999. Composition of natural, volatile-rich Na–Ca–REE–Sr carbonatitic fluids trapped in fluid inclusions. Geochim. Cosmochim. Acta 63, 3781–3797.

Carroll, M.R., Blank, J.G., 1997. The solubility of H_2O in phonolitic melts. Am. Mineral. 82, 549–556.

Cline, J.S., Bodnar, R.J., 1991. Can economic porphyry copper mineralization be generated by typical calc-alkaline melt? J. Geophys. Res. 96, 8118–8126.

Constantinescu, E., Anastasiu, N., 1979. Nepheline from the alkaline massif of Ditrău. Anal. Univ. Buc., Geol. XVIII, 15–27.

Dallmeyer, R.D., Kräutner, H.G., Neubauer, F., 1997. Middle-late Triassic $^{40}Ar/^{39}Ar$ hornblende ages for early intrusions within the Ditrău Alkaline Massif, Romania: implications for Alpine rifting in the Carpathian orogen. Geol. Carpath. (Bratisl.) 48, 347–352.

Della Ventura, G., Bellatreccia, F., Bonaccorsi, E., 2005. CO_2 in minerals of the cancrinite–sodalite group: pitiglianoite. Eur. J. Min. 17, 847–851.

Dingwell, B.D., Harris, D.M., Scarfe, C.M., 1984. The solubility of H_2O in melts in the system SiO_2–Al_2O_3–Na_2O–K_2O at 1 to 2 kbars. J. Geol. 92, 387–395.

Goldstein, R.H., Reynolds, T.J., 1994. Systematics of fluid inclusions in diagenetic minerals. Soc. Sed. Geol. Short Course, vol. 31, p. 199.

Hamilton, D.L., 1961. Nephelines as crystallization temperature indicators. J. Geol. 69, 321–329.

Hamilton, D.L., MacKenzie, W.S., 1960. Nepheline solid solution in the system $NaAlSiO_4$–$KAlSiO_4$–SiO_2. J. Petrol. 1, 56–72.

Herbich, P., 1859. Die geologishen Verhältnisse des nordwestlichen Siebenbürgens. Jahrb. Ungarn. Geol. Anst. 293–350.

Ianovici, V., 1938. Considération sur la consolidation du massif syénitique de Ditrău, en relation avec la tectonique de la région. C. R. Acad. Sci. Roum. 2, 689–694.

Jakab, Gy., 1998. Geologia Masivului Alcalin de la Ditrău. Pallas-Akad., M.-Ciuc., p. 298.

Kilinc, I.A., Burnham, C.W., 1972. Partitioning of chloride between a silicate melt and coexisting aqueous phase from 2 to 8 kbars. Econ. Geol. 67, 231–235.

Kogarko, L.N., 1974. Petrogenesis. Role of volatiles. In: Sørensen, H. (Ed.), The Alkaline Rocks. J. Wiley and Sons, London, pp. 474–487.

Kräutner, H.G., Bindea, G., 1995. The Ditrău alkaline intrusive complex and its geological environment. 3rd Symp. on Min. Guidbook to Excursion E. Buc. Rom. J. Min., vol. 77, Supl. nr. 3, p. 18.

Kräutner, H.G., Bindea, G., 1998. Timing of the Ditrău alkaline intrusive complex (Eastern Carpathians, Romania). Slovak Geol. Mag. 4, 213–221.

Lipin, V.A., 2001. Specific features of the composition of solid phases in the $Na^+K^+Ca^{2+}||CO_3^{2-}OH^-$-$H_2O$ system. Russ. J. Appl. Chem. 74, 1781–1785.

Millhollen, G.L., 1971. Melting of nepheline syenite with H_2O and H_2O+CO_2, and the effect of dilution of the aqueous phase on the beginning of melting. Am. J. Sci. 270, 244–254.

Mitchell, R.H., 1996. Classification of undersaturated and related alkaline rocks. In: Mitchell, R.H. (Ed.), Undersaturated Alkaline Rocks: Mineralogy, Petrogenesis, and Economic Potential. Mineral. Assoc. Can. Short Course, vol. 24, pp. 1–22.

Morogan, V., Lindblom, S., 1995. Volatiles associated with the alkaline-carbonatite magmatism at Alnö, Sweden: a study of fluid and solid inclusions in minerals from the Langarsholmen ring complex. Contrib. Mineral. Petrol. 122, 262–274.

Morogan, V., Upton, B.G.J., Fitton, J.G., 2000. The petrology of the Ditrău alkaline complex, Eastern Carpathians. Mineral. Petrol. 69, 227–265.

Pál-Molnár, E., 2000. Hornblendites and diorites of the Ditró szenite massif. Edited by the Dep. of Mineral., Geochem. and Petrol., Univ. of Szeged, Hungary, p. 172.

Pál-Molnár, E., Árva-Sós, E., 1995. K–Ar radiometric dating on rocks from the northern part of the Ditró szenite massif and its petrogenetic implications. Acta Mineral. Petrol. 36, 101–116 (Szeged).

Pintea, I., 1992. Fluid inclusion microthermometry and its applications in mineralogenesis. Specific examples. First Nat. Symp. on Mineral., Abstr. . Rom. J. Mineral., vol. 75, pp. 35–36.

Pintea, I., Diamond, L.W., 1994. Immiscible, hypersaline CO_2–H_2O fluids associated with REE and MoS_2 mineralization in the Ditrău alkaline massif, Transylvania, Romania. IMA 16th Gen. Meet. 4–6 Sept., Pisa, Abstr., pp. 328–329.

Platt, R.G., 1996. Nepheline syenite complexes — an overview. In: Mitchell, R.H. (Ed.), Undersaturated Alkaline Rocks: Mineralogy, Petrogenesis, and Economic Potential. Mineral. Assoc. Can. Short Course, vol. 24, pp. 63–99.

Potter, J., Rankin, A.H., Treloar, P.j., 2004. Abiogenic Fischer–Tropsch synthesis of hydrocarbon in alkaline igneous rocks; fluid inclusion, textural and isotopic evidence from the Lovozero complex, N.W. Russia. Lithos 75, 311–330.

Preece III, R.K., Beane, R.E., 1982. Contrasting evolutions of hydrothermal alteration in quartz monzonite and quartz diorite wall rocks at the Sierrita porphyry copper deposit, Arizona. Econ. Geol. 77, 1621–1641.

Roedder, E., Bodnar, R.J., 1980. Geologic pressure determinations from fluid inclusion studies. Annu. Rev. Earth Planet. Sci. 8, 263–301.

Săndulescu, M., 1975. Essai de synthése structurale des Carpathes. Bull. Soc. Geol. France, Paris, Ser., vol. 7, 17/3, pp. 299–358.

Shinohara, H., Iiyama, J.T., Matsuo, S., 1989. Partition of chlorine compounds between silicate melt and hydrothermal solutions: I. Partition of NaCl–KCl. Geochim. Cosmochim. Acta 53, 2617–2630.

Signorelli, S., Carroll, M.R., 2000. Solubility and fluid-melt partitioning of Cl in hydrous phonolitic melts. Geochim. Cosmochim. Acta 64, 2851–2862.

Sîrbescu, M., Jenkins, D.M., 1999. Experiments on the stability of cancrinite in the system Na_2O–CaO–Al_2O_3–SiO_2–CO_2–H_2O. Am. Mineral. 84, 1850–1860.

Sobolev, V.S., Bazarova, T.Yu., Kostyuk, V.P., 1974. Inclusions in the minerals of some types of alkaline rocks. In: Sørensen, H. (Ed.), The Alkaline Rocks. J. Wiley and Sons, London, pp. 389–401.

Sørensen, H., 1974. The Alkaline Rocks. J. Wiley and Sons, London, p. 622.

Sterner, S.M., Bodnar, R.J., 1984. Synthetic fluid inclusions in natural quartz. I. Compositional types synthesized and applications to experimental geochemistry. Geochim. Cosmochim. Acta 48, 2659–2668.

Sterner, S.M., Hall, D.L., Bodnar, R.J., 1988. Synthetic fluid inclusions. V. Solubility relations in the system NaCl–KCl–H_2O under vapor-saturated conditions. Geochim. Cosmochim. Acta 52, 989–1005.

Streckeisen, A., 1938. Das Nephelinsyenit-Massiv von Ditró (Rumänien) als Beispiel einer kombinierten Differentiation und Assimilation. Verh. Schweiz. Nat. Forsch. Ges., 159–161.

Streckeisen, A., 1960. On the structure and the origin of the nepheline syenite complex of Ditró (Transylvania). 21th IGC, vol. 13, pp. 228–238.

Streckeisen, A., Hunziker, J.C., 1974. On the origin and age of the nepheline–syenite complex of Ditró (Transylvania, Rumania). Schweiz. Mineral. Petrol. Mitt. 54, 59–77.

Student, J.J., Bodnar, R.J., 1999. Synthetic fluid inclusions XIV: Microthermometric and compositional analysis of coexisting silicate melt and aqueous fluid inclusions trapped in the haplogranite–H_2O–NaCl–KCl system at 800 °C and 2000 bars. J. Petrol. 40, 1509–1525.

Student, J.J., Bodnar, R.J., 2004. Silicate melt inclusions in porphyry copper deposits: identification and homogenization behavior. Can. Mineral. 42, 1563–1600.

Tilley, C.E., 1954. Nepheline-alkali feldspar paragenesis. Am. J. Sci. 252, 65–75.

Webster, J.D., 2004. The exsolution of magmatic hydrosaline chloride liquids. Chem. Geol. 210, 33–48.

Zirkel, F., 1866. Lehrbuch der Petrographie, Bd., vol. 1. Marcus Verlag, Bonn, p. 607.